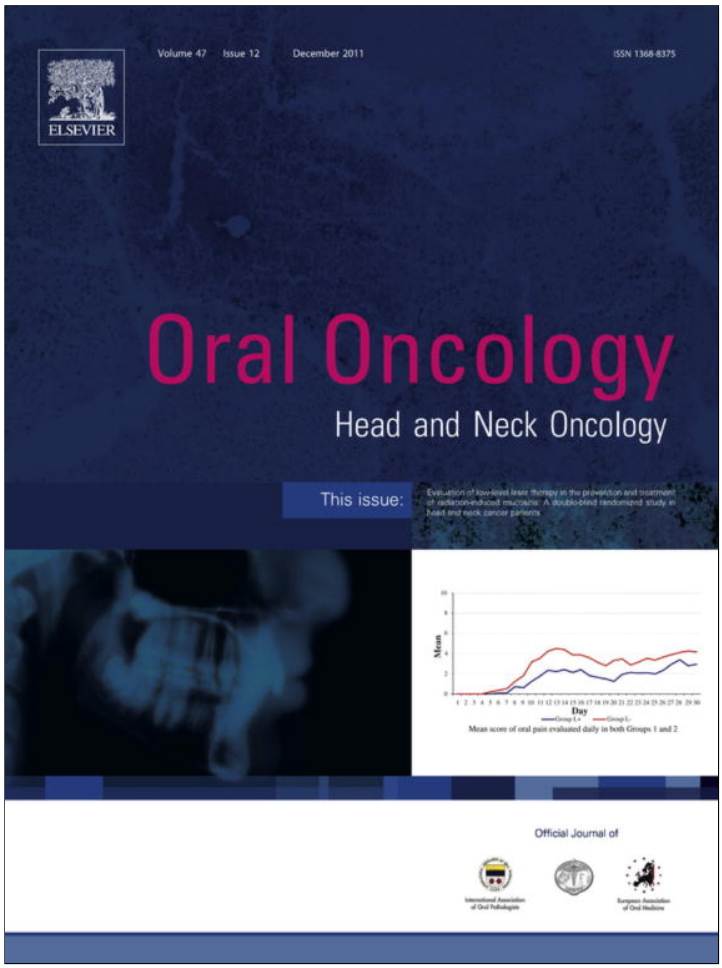

Oral Oncology 47 (2011) 1127–1133

Contents lists available at SciVerse ScienceDirect

Oral Oncology

journal homepage: www.elsevier.com/locate/oraloncology

Antitumor activity of a novel histone deacetylase inhibitor (*S*)-HDAC42 in oral squamous cell carcinoma

Li-Yuan Bai [a,c], Chang-Fang Chiu [a,b], Shiow-Lin Pan [f], Aaron M. Sargeant [g], Tzong-Ming Shieh [d], Ying-Chu Wang [e], Jing-Ru Weng [e,*]

[a] *Division of Hematology and Oncology, Department of Internal Medicine, China Medical University Hospital, Taichung 40402, Taiwan*
[b] *Cancer Center, China Medical University Hospital, Taichung 40402, Taiwan*
[c] *College of Medicine, China Medical University, Taichung 40402, Taiwan*
[d] *Department of Dental Hygiene, China Medical University, Taichung 40402, Taiwan*
[e] *Department of Biological Science and Technology, China Medical University, Taichung 40402, Taiwan*
[f] *Division of Biotechnology and Pharmaceutical Research, National Health Research Institutes, Zhunan 35053, Taiwan*
[g] *Charles River Laboratories, Preclinical Services, Spencerville, OH 45887, USA*

ARTICLE INFO

Article history:
Received 8 February 2011
Received in revised form 27 July 2011
Accepted 28 July 2011
Available online 23 August 2011

Keywords:
Oral cancer
(*S*)-HDAC42
Histone deacetylase inhibitor
Akt
NF-κB

SUMMARY

The aberrant regulation of epigenetic systems including histone acetylation contributes to inappropriate gene expression in cancer cells. In this study, we investigated the antitumor effects of the novel histone deacetylase inhibitor (*S*)-HDAC42 in oral squamous cell carcinoma (OSCC) cells. The antiproliferative effect of (*S*)-HDAC42 was multifold higher than that of suberoylanilide hydroxamic acid in a panel of oral squamous carcinoma cell lines examined. (*S*)-HDAC42 mediated caspase-dependent apoptosis by targeting multiple signaling pathways relevant to cell cycle progression and survival. We demonstrated that (*S*)-HDAC42 downregulated the levels of phospho-Akt, cyclin D1, and cyclin-dependent kinase 6, accompanied by increased p27 and p21 expression. In addition, (*S*)-HDAC42 suppressed NF-κB signaling by blocking tumor necrosis factor-α-induced nuclear translocation, and activated reactive oxygen species generation. Finally, (*S*)-HDAC42 exhibited high potency in suppressing OSCC tumor growth in a Ca922 xenograft nude mouse model. Together, these findings underscore the translational value of (*S*)-HDAC42 in fostering new therapeutic strategies for OSCC.

Introduction

Squamous oral cell carcinoma (OSCC) is the most commonly diagnosed oral cancer. Although the etiologies underlying the development of OSCC are not fully understood, tobacco use, alcohol, and betel quid chewing are major risk factors. The main treatment modalities include radical surgery followed by chemoradiation, and definitive chemoradiation. However, the prognosis is poor for relapsed and refractory disease or for patients with metastatic disease even after therapeutic inventions with chemotherapeutic or targeted agents.[1] This predicament highlights the necessity to develop novel therapeutic strategies for patients with advanced OSCC.

Aberrant epigenetic regulation has been shown to lead to inappropriate gene expression, a key event in the pathogenesis of many types of cancer.[2,3] Accordingly, compounds modulating epigenetic machinery represent a key area of focus in cancer therapeutic development. For example, histone deacetylase (HDAC) inhibitors have been shown to suppress cell proliferation,[4] induce apoptosis,[5,6] autophagy,[7] or senescence[8] in different cancer cells.

(*S*)-HDAC42 is a phenylbutyrate-based HDAC inhibitor with high antitumor efficacy against various types of cancers.[9–13] Evidence suggests that (*S*)-HDAC42 mediates antitumor effects through both histone acetylation-dependent and -independent mechanisms.[10,14] From a mechanistic perspective, this broad spectrum of antitumor mechanisms underlies the high potency of (*S*)-HDAC42 in suppressing cancer cell growth *in vitro* and *in vivo*.[9–13]

In the present study, we report the *in vitro* and *in vivo* antitumor efficacy of (*S*)-HDAC42 in OSCC cells through the interference of multiple signaling pathways relevant to cell cycle progression and survival, including those regulated by Akt, nuclear factor-kappa B (NF-κB), and reactive oxygen species (ROS).

Materials and methods

Cells and culture conditions

The OSCC cell lines Ca922, SAS, and HSC-3 were obtained from Japanese Collection of Research Bioresources (Tokyo, Japan). Ca922

* Corresponding author. Address: 91 Hsueh-Shih Road, Taichung 404, Taiwan. Tel.: +886 4 22053366x2511; fax: +886 4 22071507.
E-mail address: columnster@gmail.com (J.-R. Weng).

1368-8375/$ - see front matter © 2011 Elsevier Ltd. All rights reserved.
doi:10.1016/j.oraloncology.2011.07.031

cells were cultured in MEM (Invitrogen, Carlsbad, CA); SAS and HSC-3 cells were cultured in DMEM (Invitrogen). All culture medium were supplemented with 10% heat-inactivated fetal bovine serum (FBS, Gibco, Grand Island, NY) and penicillin (100 U/ml)/streptomycin (100 μg/ml) (Invitrogen). Normal human oral keratinocytes (NHOK) were kindly provided by Dr. Yuan-Chien Chen (China Medical University Hospital) and maintained in the keratinocyte serum-free medium (Gibco, Grand Island, NY). All cell types were cultured at 37 °C in an atmosphere of 5% CO_2.

Reagents

(*S*)-HDAC42 [(*S*)-(+)-*N*-hydroxy-4-(3-methyl-2-phenylbutyrylamino) benzamide] and suberoylanilide hydroxamic acid (SAHA) were synthesized as previously reported,[10] and the identity and purity were confirmed by nuclear magnetic resonance and mass spectrometry.

MTT assay

Cell viability was assessed by 3-(4,5-dimethylthiazol-2-yl)-2,5-diphenyltetrazolium bromide (MTT) assays in six replicates. After drug treatment, MTT (0.5 mg/ml) was added to each well and cells were incubated at 37 °C for 2 h. Reduced MTT was dissolved in DMSO (200 μL/well), and the absorbance was measured at 570 nm.

TUNEL assay

Cells (5×10^5) were cultured in 6-well plates in medium containing 5% FBS with or without drug treatment. Apoptotic cells were stained using the APO-Brdu™ TUNEL assay kit (Invitrogen) for 30 min at 37 °C, fixed for 30 min in 70% ethanol, and analyzed by fluorescence microscopy.

Flow cytometry

For assessment of apoptosis, cells were stained with Annexin V-FITC and propidium iodide according to the vendor's protocols (BD Pharmingen, San Diego). Caspase-3 activation was assessed using a FITC rabbit anti-active caspase-3 kit (BD Pharmingen) according the manufacturer's protocol. ROS production was detected using the fluorescence probe 5-(and-6)-carboxy-2′,7′-dichloro-dihydrofluorescein diacetate (carboxy-DCFDA). Data were analyzed by ModFitLT V3.0 software program.

Immunoblotting

Cell lysates were prepared using RIPA buffer (150 mM NaCl, 50 mM Tris PH 8.0, 1% NP40, 0.5% sodium deoxycholate and 0.1% sodium dodecyl sulfate) in the presence of a cocktail of protease inhibitors (Sigma–Aldrich, St. Louis, MO) and phosphatase inhibitors (Calbiochem, Gibbstown, NJ). Antibodies against various proteins were obtained from the following sources: p-Akt (Ser473), p-Akt (Thr308) (Santa Cruz Biotechnology, Santa Cruz, CA), α-tubulin, poly-ADP-ribose polymerase (PARP), HDAC1, HDAC4, p-IκBα, IκBα, Akt, NF-κB, caspase-9, p27, cyclin D1, CDK6, GAPDH (Cell signaling; Beverly, MA), procaspase-8, p21 (Abcam Inc., Cambrige, MA), acetyl-histone H3, and HDAC3 (Upstate, Temecula, CA). The goat anti-rabbit IgG-horseradish peroxidase (HRP) conjugates and goat anti-mouse IgG-HRP conjugates were purchased from Perkin-Elmer life Sciences, Inc. (Boston, MA).

Confocal imaging of NF-κB nuclear localization

Cells (1×10^5/3 mL) were plated on cover slips in each well of six-well plates, incubated in medium with or without (*S*)-HDAC42 for 48 h, followed by 10 ng/mL tumor necrosis factor-α (TNF-α) for 30 min. The cells were then fixed in 2% paraformaldehyde for 30 min at room temperature, and permeabilized with 0.1% Triton X-100 for 20 min. After blocking with 1% bovine serum albumin (BSA), cells were incubated with a rabbit anti-human NF-κB antibody overnight at 4 °C, followed by anti-rabbit IgG, washed, and subjected to confocal microscopy.

In vivo efficacy of (S)-HDAC42 in an OSCC xenograft tumor model

Twelve female nude mice of 5–7 weeks of age were obtained from the National Laboratory Animal Center (Taipei, Taiwan). Ca922 cells were cultured in MEM supplemented with 10% heat-inactivated FBS. Each mouse was inoculated subcutaneously with 1×10^7 Ca922 cells in 0.1 ml phosphate-buffered saline. Tumor diameter was measured twice weekly using calipers and the tumor volume was calculated using a standard formula: width^2 × length × 0.52. Body weights of the mice were measured once weekly. When the mean tumor volume reached 60 mm^3, mice were randomized into two groups ($n = 6$). Mice in the treatment group received (*S*)-HDAC42 orally at a dose of 25 mg/kg per day, and those in the control group received the methylcellulose/Tween 80 vehicle. All mice received treatments by gavage (10 μL/g body weight) daily till reaching the endpoint. The criteria for endpoint included death, body weight loss more than 30% or tumor size more than 1200 mm^3. The *in vivo* experiment protocol was

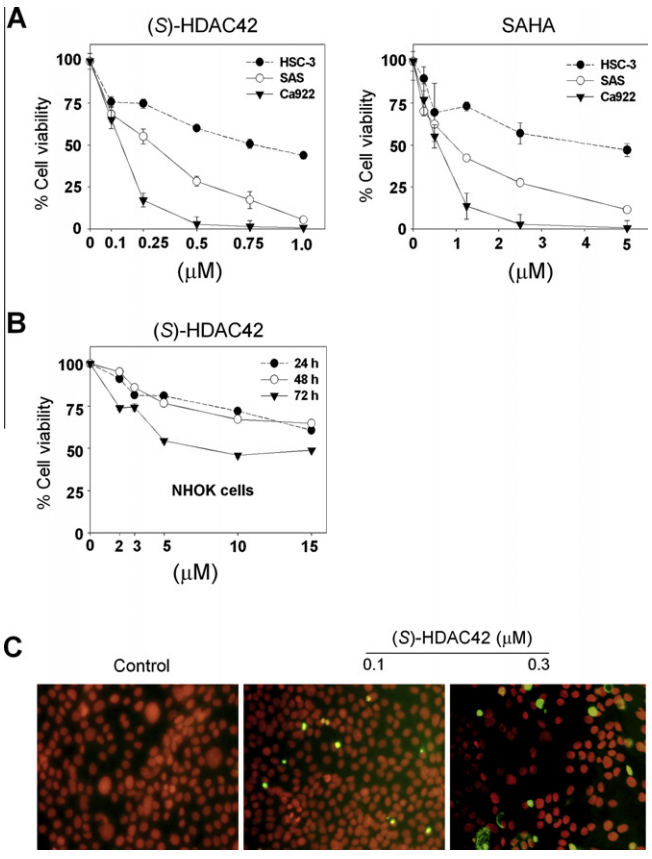

Figure 1 The cytotoxic effect of (*S*)-HDAC42 and suberoylanilide hydroxamic acid (SAHA) in oral cancer cells and normal human oral keratinocytes (NHOK). Antiproliferative effect of (*S*)-HDAC42 and SAHA in three different oral cancer cell lines (A). Cells were exposed to (*S*)-HDAC42 or SAHA at the indicated concentrations for 48 h, and cell viability was assessed by MTT assay ($n = 6$). NHOK were relatively insensitive to (*S*)-HDAC42 (B). TUNEL assay in Ca922 cells treated with (*S*)-HDAC42 for 48 h (C). The green color in TUNEL stain denotes DNA fragmentation. (For interpretation of the references to colour in this figure legend, the reader is referred to the web version of this article.)

approved by the Animal Ethical Review Committee at National Taiwan University.

Statistical analysis

Experiments were performed at least in triplicate and results are represented as means ± standard deviation (SD) except indicated otherwise. For evaluating caspase-3 activation and ROS production, the Student's *t*-test was used. In the *in vivo* study, a Log rank test was used for assessing the effect of (*S*)-HDAC42 on tumor growth and for analyzing the difference of time to endpoint. A Student's *t*-test was also used to compare the difference in body weight with regards to day on treatment. In all experiments, a *p* value less than 0.05 was considered statistically significant.

Results

(S)-HDAC42 mediates greater cytotoxicity than SAHA in OSCC cell lines

The antiproliferative effect of (*S*)-HDAC42 and SAHA was assessed using MTT assays in three OSCC cell lines, HSC-3, SAS and Ca922. Cells (2×10^5/mL) were exposed to (*S*)-HDAC42 and SAHA at the concentration range of 0.1–1 and 1–5 μM, respectively, both of which showed a dose-dependent decrease in cell viability. Relative to SAHA, (*S*)-HDAC42 was consistently more potent in these OSCC cell lines (Fig. 1A). The IC_{50} values of (*S*)-HDAC42 and SAHA to suppress the viability of Ca922, SAS, and HSC-3 cells at 48 h of treatment were 0.16, 0.29, and 0.79 μM, respectively, and 0.72, 1.12, and 3.25 μM, respectively. The IC_{50} values at 24 h were higher than those at 48 h (data not shown). Therefore, we treated cells with DMSO or (*S*)-HDAC42 for 48 h in the following experiments. Importantly, normal human oral keratinocytes were much less sensitive to (*S*)-HDAC42 (Fig. 1B). TUNEL assays indicated a greater extent of DNA fragmentation in Ca922 cells in response to (*S*)-HDAC42 vis-à-vis vehicle control (Fig. 1C), suggesting the role of apoptosis in (*S*)-HDAC42-mediated cytotoxicity.

(S)-HDAC42 mediates apoptotic death

We obtained several lines of evidence that (*S*)-HDAC42-mediated cell death was attributable to apoptosis. As shown, flow cytometry indicated a dose-dependent effect of (*S*)-HDAC42 on increasing the proportion of apoptotic cells (defined as annexin V+ cells) in all three cell lines (Fig. 2A). Furthermore, Western blot

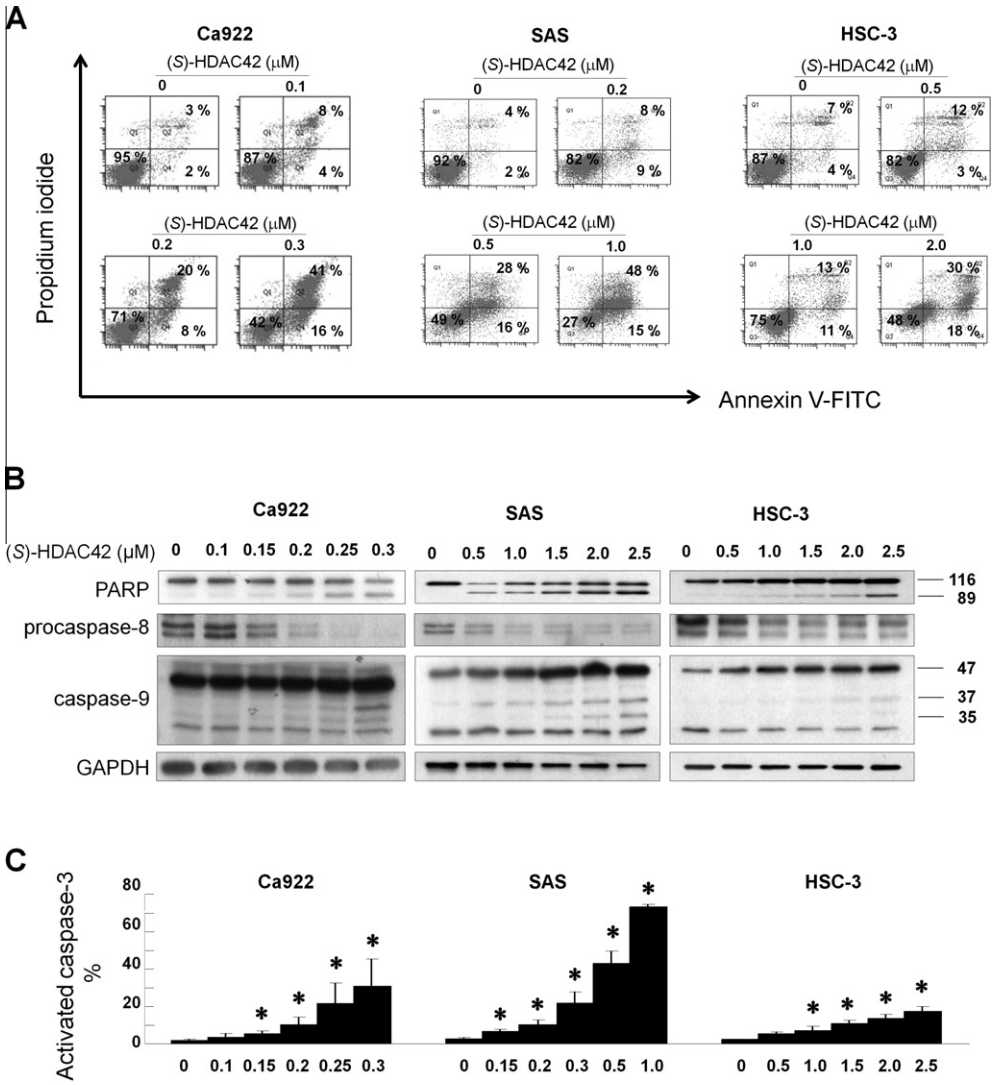

Figure 2 (*S*)-HDAC42 induced apoptosis and caspase activation. Annexin V-FITC/propodium iodide analysis of apoptosis in three oral cancer cell lines treated with (*S*)-HDAC42 for 48 h (A). Western blotting analysis of PARP, procaspase-8 and caspase-9 in cells treated with (*S*)-HDAC42 for 48 h (B). (*S*)-HDAC42 induced a dose-dependent increase of activated caspase-3 (C, $n = 3$). * Denotes $p < 0.05$ when compared with the control group.

analysis showed that (*S*)-HDAC42 induced PARP cleavage and caspase-8 and -9 activation in a dose-dependent manner (Fig. 2B). To further confirm the involvement of caspase activation in (*S*)-HDAC42-mediated apoptosis, cells treated with indicated concentrations of (*S*)-HDAC42 or DMSO were analyzed for activated caspase-3 expression by flow cytometry (Fig. 2C). Treatment with (*S*)-HDAC42 for 48 h induced incremental levels of activated caspase-3, from 1.8% in the control group to 5.6%, 10.5%, 21.8%, and 30.9% in Ca922 cells treated with 0.15, 0.2, 0.25, and 0.3 μM of (*S*)-HDAC42, respectively ($p = 0.013$, 0.021, 0.034, and 0.025 compared to the control group). The activated caspase-3 was 6.8%, 10.4%, 22.1%, 43.0%, and 73.4% in SAS treated with 0.15, 0.2, 0.3, 0.5, and 1.0 μM of (*S*)-HDAC42, respectively ($p = 0.006$, 0.023, 0.024, 0.007, and 0.0002 compared to the control group). For HSC-3, the activated caspase-3 was 10.9%, 13.7%, 17.5%, and 19.1% in cells treated with 1.0, 1.5, 2.0 and 2.5 μM of (*S*)-HDAC42, respectively ($p = 0.023$, 0.014, 0.012 and 0.010 compared to the control group). These results support that (*S*)-HDAC42 induces caspase-dependent apoptosis in Ca922 cells.

Effects of (S)-HDAC42 on markers related to HDAC inhibition and the activation/expression status of Akt and NF-κB

To demonstrate the activity of (*S*)-HDAC42 on HDAC inhibition, oral cancer cells (2×10^5/mL) were treated with (*S*)-HDAC42 for 48 h. HDAC inhibition was evidenced by increased acetylation levels of histone H3 in a concentration-dependent manner (Fig. 3A). It is noteworthy that (*S*)-HDAC42 not only affected the activity, but also caused dose-dependent downregulation of the expression of HDAC1, HDAC3 and HDAC4 in Ca922, the most sensitive cells, and to a lesser extent, HDAC1 and HDAC4 in SAS cells.

To investigate other mechanisms that might underlie the apoptotic effect of (*S*)-HDAC42, (*S*)-HDAC42-treated oral cancer cell lysates were also blotted with antibodies against signaling proteins involved in the regulation of cell survival and cell cycle progression. (*S*)-HDAC42 dose-dependently reduced the phosphorylation levels of Akt (Fig. 3B). The upregulation of the CDK inhibitors p21 and p27 has been reported to be a hallmark feature of HDAC inhibition.[9,15] As shown, (*S*)-HDAC42 induced a dose-dependent increase in the expression of p27 and p21. Moreover, our data indicate the unique ability of (*S*)-HDAC42 in suppressing the expression of other cell cycle-regulatory proteins, including CDK6 and cyclin D1.

As NF-κB signaling is a key pathway targeted by HDAC inhibitors in several types of cancer cells,[9,16,17] we analyzed the spatial change of NF-κB by confocal microscopy in drug-treated Ca922, SAS, and HSC-3 cells (Fig. 3C). NF-κB, located in the cytoplasm of cells treated with DMSO, redistributed to the nuclei when the cells were treated with 10 ng/mL of TNF-α. Treatment with (*S*)-HDAC42 at a concentration of 0.17, 0.1, and 1.5 μM in Ca922, SAS and HSC-3 cells for 48 h prohibited the activation and subsequent nuclear translocation of NF-κB.

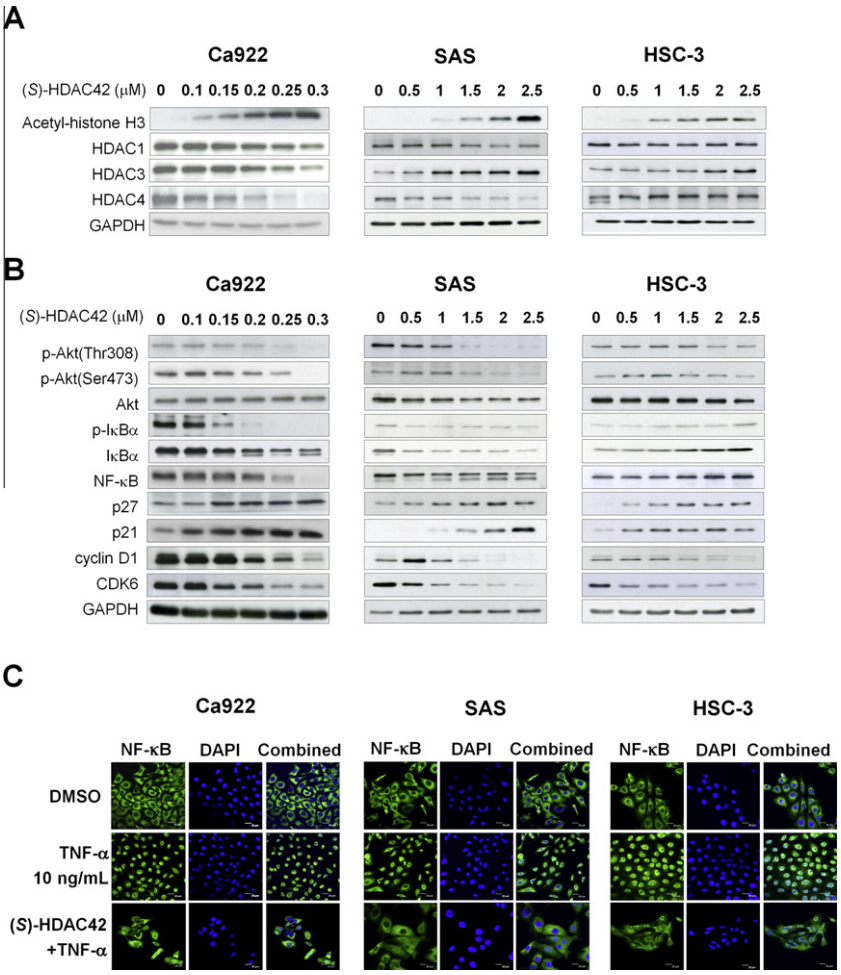

Figure 3 Effects of (*S*)-HDAC42 on HDAC inhibition, Akt and NF-κB pathway proteins, and cell cycle-related proteins in oral cancer cells treated with (*S*)-HDAC42 for 48 h (A and B). Confocal microscopic examination of the spatial change of NF-κB in cells treated with TNF-α with or without (*S*)-HDAC42 (C). TNF-α (10 ng/mL) for 30 min induced activation and nuclear translocation of NF-κB which was inhibited by pretreatment of (*S*)-HDAC42 for 48 h. The concentration of (*S*)-HDAC42 used was 0.17, 0.1 and 1.5 μM for Ca922, SAS and HSC-3, respectively.

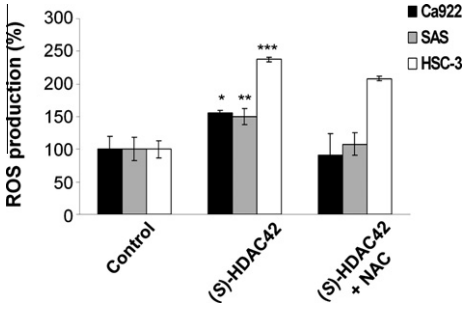

Figure 4 (*S*)-HDAC42 induced reactive oxygen species (ROS) generation. Oral cancer cells (2×10^5/3 mL) were treated with DMSO or (*S*)-HDAC42 with or without *N*-acetylcysteine (NAC) for 48 h. The ROS production in each condition is expressed as percentage of that in the control group. $^{*}p = 0.0185$, $^{**}p = 0.032$ and $^{***}p = 0.0006$, when compared with the control group.

(S)-HDAC42 increases ROS production

Increased ROS has been reported to be responsible for the activity of some anticancer drugs.[18] Thus we examined the level of ROS in oral cancer cells treated with (*S*)-HDAC42 using a flow cytometry. (*S*)-HDAC42 significantly increased ROS generation by 55%, 50%, and 137% compared to the control group in Ca922, SAS, and HSC-3, respectively ($^{*}p = 0.0185$, $^{**}p = 0.032$, and $^{***}p = 0.0006$, Fig. 4). Co-treatment with an antioxidant *N*-acetylcysteine either prohibited or decreased the (*S*)-HDAC42-mediated increase in ROS production.

(S)-HDAC42 slows growth of Ca922 xenografts and prolongs the survival of tumor-bearing athymic nude mice

As shown in Fig. 5A, (*S*)-HDAC42 significantly inhibited Ca922 xenograft tumor growth by 65% on day 20 compared to vehicle-treated mice ($p < 0.05$). The mean tumor volume on day 20 was 383 and 1090 mm^3 for (*S*)-HDAC42- and vehicle-treated mice, respectively. In addition to inhibiting growth of xenograft tumors, (*S*)-HDAC42 significantly prolonged the survival time of mice (Fig. 5B). The median time to endpoint was 19 and 31 days for vehicle and compound-treated groups, respectively. Although the body weight loss of mice treated with (*S*)-HDAC42 did not reach the criteria for early sacrifice (30% decrease), it was statistically significant compared with that of mice of the control group beginning on day 7 of treatment ($p = 0.02$) (Fig. 5C).

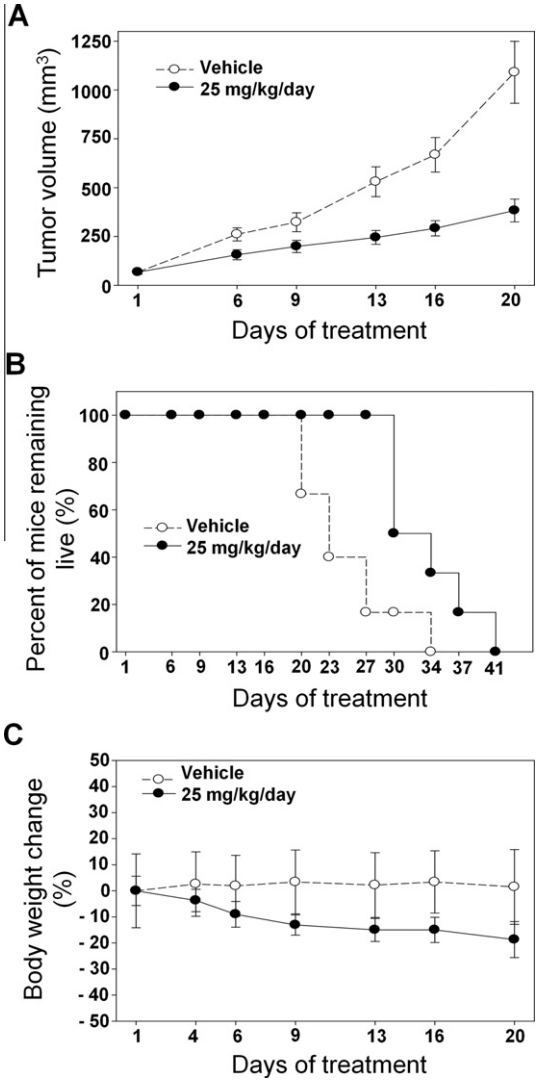

Figure 5 Effect of (*S*)-HDAC42 on the growth of Ca922 xenograft and on the survival time of tumor-bearing nude mice. Nude mice were treated with (*S*)-HDAC42 or vehicle orally once daily (six mice per group) and tumor diameter was measured twice weekly. Growth curve of Ca922 xenograft tumors (A). Survival time to endpoint of xenograft study (B). The median time to endpoint was 19 and 31 days for vehicle- and (*S*)-HDAC42-treated groups, respectively. Body weight change of mice (C).

Discussion

Epigenetic changes have been shown to play a key role in oral carcinogenesis through the dysregulation of the expression of oncogenes and/or tumor suppressor genes.[19,20] For example, the HDAC inhibitor FR901228 caused the reactivation of the mapsin tumor suppressor gene expression.[21] In addition, HDAC inhibitors have also been shown to prevent radiation-induced oral mucositis and to inhibit chemical-induced oral carcinogenesis in a hamster model,[22] which was correlated with the suppression of oncomiRs and Rad51 overexpression, the upregulation of differentiation markers and the decrease of intracellular HDAC activity and oxidative stress. These *in vitro* and *in vivo* data suggest the translational potential of HDAC inhibitors in oral cancer treatment. In our study, (*S*)-HDAC42 reduced oral tumor growth in a xenograft mouse model and prolonged the median survival of tumor-bearing mice in the absence of limiting toxicity.

In addition to inhibiting HDACs, (*S*)-HDAC42 also caused the downregulation of Akt phosphorylation and NF-κB activity, and modulated the expression levels of several cell cycle-regulatory proteins in OSCC cells. It has been demonstrated that Akt inhibition could induce the mesenchymal-to-epithelial reverting transition through the downregulation of Snail and Twist in OSCC, suggesting Akt as a target for controlling cancer metastasis.[23] NF-κB is another important target for anti-oral cancer therapy since, compared with normal epithelial cells, oral cancer cells usually express higher constitutive NF-κB levels which contribute to a malignant phenotype.[24,25] NF-κB also regulates the expression of many genes that are important for cell protection from radiation and chemotherapy, anti-apoptosis, cell survival, tumorigenesis, and cancer metastasis.[26,27] By down regulating the NF-κB pathway, bortezomib and Trichostatin A have been shown to effectively inhibit the cell growth of head and neck squamous cell carcinoma.[28] The concerted actions of acetylation-dependent and acetylation-independent effects of (*S*)-HDAC42, which were reported in other cancer cells previously,[9,12,22] are considered to be important for the anti-tumor activity of (*S*)-HDAC42 in oral cancer.

Increased ROS is implicated in inflammation, cardiovascular disease, stroke, aging process, and cell apoptosis.[29] Recent cumula-

tive evidences implicate ROS generation as an effective strategy in antitumor therapy as well.[18] The HDAC inhibitor LAQ-824 was shown to induce increased ROS, mitochondrial injury and apoptosis in human leukemia cells (blocked by *N*-acetylcysteine).[30] Besides the direct cytotoxicity, LAQ-824 accentuated fludarabine lethality by ROS generation and modulation of DNA repair processes in leukemia cells.[31] PDX101, another HDAC inhibitor, potentiated a bortezomib-induced anti-myeloma effect by inducing oxidative stress and ROS-mediated DNA damage.[32] Not reported in previous studies of (*S*)-HDAC42, our study showed that (*S*)-HDAC42 increases ROS generation which could be rescued by co-treatment with *N*-acetylcysteine in Ca922 and SAS cells. (*S*)-HDAC42 induced the highest ROS production in HSC-3 cells which was partially rescued by *N*-acetylcysteine. This induction of ROS is noteworthy because it may represent one of the antitumor mechanisms of HDAC inhibitors.

Data from previous studies suggest that (*S*)-HDAC42 has the following advantages in addition to the aforementioned pleiotropic effect. First, it has a lower IC_{50} than SAHA in suppressing the growth of tumor cells.[9,10] This higher potency is also exemplified in the present oral cancer study. Second, mice have been shown to tolerate the therapeutic range of (*S*)-HDAC42 well without overt signs of toxicity.[10–13,33] The therapeutic efficacy of (*S*)-HDAC42 is demonstrated in the present study by the significant delay in tumor growth and prolonging of the time to endpoint of the xenograft experiment. The median time to tumor size greater than 1200 mm^3 was 19 and 31 days for vehicle and (*S*)-HDAC42-treated mice, respectively.

Preclinical changes of (*S*)-HDAC42 with seemingly acceptable risk: benefit ratios have included reversible testicular and thymic atrophy and leukopenia; however, mortality and significant effects on body weight after repeated oral administration in the previous studies were lacking.[10,12] Accordingly, the loss of body weight in the present study was unexpected, and the real impact of (*S*)-HDAC42 on body weight should be clarified in future studies. Importantly, a contributing effect of body weight loss on delayed growth of the OSCC xenograft tumors, in addition to the pleiotropic anticancer activity of (*S*)-HDAC42, could not be completely ruled out.

In conclusion, (*S*)-HDAC42 has promising antitumor activities against oral cancer cells *in vivo* and *in vitro*. It induces apoptosis in oral cancer cells through HDAC inhibition, downregulation of Akt and NF-κB signaling and modulation of cell cycle-related proteins. The xenograft mouse model shows its effect on slowing the growth of oral cancer. Further studies are warranted to validate the effect of (*S*)-HDAC42 in oral cancer clinically.

Role of the funding source

The sponsors have no role in study design, collection, analysis and interpretation of data; in the writing of the manuscript; and in the decision to submit the manuscript.

Conflict of interest statement

The authors declare no competing financial interests.

Acknowledgements

This work was supported in part by Grants from the Taiwan Department of Health, China Medical University Hospital Cancer Research of Excellence (DOH100-TD-C-111-005), National Science Council Grant (NSC 99-2320-B-039-007-MY2) and China Medical University (CMU95-304, CMU97-101, CMU97-082, DMR-97-017, DMR-97-021).

References

1. Vermorken JB, Remenar E, van Herpen C, Gorlia T, Mesia R, Degardin M, et al. Cisplatin, fluorouracil, and docetaxel in unresectable head and neck cancer. *N Engl J Med* 2007;**357**:1695–704.
2. Huang L. Targeting histone deacetylases for the treatment of cancer and inflammatory diseases. *J Cell Physiol* 2006;**209**:611–6.
3. Lin HY, Chen CS, Lin SP, Weng JR. Targeting histone deacetylase in cancer therapy. *Med Res Rev* 2006;**26**:397–413.
4. Johnstone RW. Histone-deacetylase inhibitors: novel drugs for the treatment of cancer. *Nat Rev Drug Discov* 2002;**1**:287–99.
5. Lindemann RK, Gabrielli B, Johnstone RW. Histone-deacetylase inhibitors for the treatment of cancer. *Cell Cycle* 2004;**3**:779–88.
6. Bhalla KN. Epigenetic and chromatin modifiers as targeted therapy of hematologic malignancies. *J Clin Oncol* 2005;**23**:3971–93.
7. Shao Y, Gao Z, Marks PA, Jiang X. Apoptotic and autophagic cell death induced by histone deacetylase inhibitors. *Proc Natl Acad Sci USA* 2004;**101**:18030–5.
8. Xu WS, Perez G, Ngo L, Gui CY, Marks PA. Induction of polyploidy by histone deacetylase inhibitor: a pathway for antitumor effects. *Cancer Res* 2005;**65**:7832–9.
9. Bai LY, Omar HA, Chiu CF, Chi ZP, Hu JL, Weng JR. Antitumor effects of (*S*)-HDAC42, a phenylbutyrate-derived histone deacetylase inhibitor, in multiple myeloma cells. *Cancer Chemother Pharmacol* 2011;**68**:489–96.
10. Kulp SK, Chen CS, Wang DS, Chen CY. Antitumor effects of a novel phenylbutyrate-based histone deacetylase inhibitor, (*S*)-HDAC-42, in prostate cancer. *Clin Cancer Res* 2006;**12**:5199–206.
11. Lu YS, Kashida Y, Kulp SK, Wang YC, Wang D, Hung JH, et al. Efficacy of a novel histone deacetylase inhibitor in murine models of hepatocellular carcinoma. *Hepatology* 2007;**46**:1119–30.
12. Sargeant AM, Rengel RC, Kulp SK, Klein RD, Clinton SK, Wang YC, et al. OSU-HDAC42, a histone deacetylase inhibitor, blocks prostate tumor progression in the transgenic adenocarcinoma of the mouse prostate model. *Cancer Res* 2008;**68**:3999–4009.
13. Yang YT, Balch C, Kulp SK, Mand MR, Nephew KP, Chen CS. A rationally designed histone deacetylase inhibitor with distinct antitumor activity against ovarian cancer. *Neoplasia* 2009;**11**:552–63.
14. Chen CS, Weng SC, Tseng PH, Lin HP, Chen CS. Histone acetylation-independent effect of histone deacetylase inhibitors on Akt through the reshuffling of protein phosphatase 1 complexes. *J Biol Chem* 2005;**280**:38879–87.
15. Zhu P, Huber E, Kiefer F, Gottlicher M. Specific and redundant functions of histone deacetylases in regulation of cell cycle and apoptosis. *Cell Cycle* 2004;**3**:1240–2.
16. Carlisi D, Lauricella M, D'Anneo A, Emanuele S, Angileri L, Di Fazio P, et al. The histone deacetylase inhibitor suberoylanilide hydroxamic acid sensitises human hepatocellular carcinoma cells to TRAIL-induced apoptosis by TRAIL-DISC activation. *Eur J Cancer* 2009;**45**:2425–38.
17. Usami M, Kishimoto K, Ohata A, Miyoshi M, Aoyama M, Fueda Y, et al. Butyrate and trichostatin A attenuate nuclear factor kappaB activation and tumor necrosis factor alpha secretion and increase prostaglandin E2 secretion in human peripheral blood mononuclear cells. *Nutr Res* 2008;**28**:321–8.
18. Fang J, Seki T, Maeda H. Therapeutic strategies by modulating oxygen stress in cancer and inflammation. *Adv Drug Deliv Rev* 2009;**61**:290–302.
19. Esteller M. Epigenetics in cancer. *N Engl J Med* 2008;**358**:1148–59.
20. Taby R, Issa JP. Cancer epigenetics. *CA Cancer J Clin* 2010;**60**:376–92.
21. Murakami J, Asaumi J, Maki Y, Tsujigiwa H, Kuroda M, Nagai N, et al. Effects of demethylating agent 5-aza-2(′)-deoxycytidine and histone deacetylase inhibitor FR901228 on maspin gene expression in oral cancer cell lines. *Oral Oncol* 2004;**40**:597–603.
22. Chung YL, Lee MY, Pui NN. Epigenetic therapy using the histone deacetylase inhibitor for increasing therapeutic gain in oral cancer: prevention of radiation-induced oral mucositis and inhibition of chemical-induced oral carcinogenesis. *Carcinogenesis* 2009;**30**:1387–97.
23. Hong KO, Kim JH, Hong JS, Yoon HJ, Lee JI, Hong SP, et al. *J Exp Clin Cancer Res* 2009;**28**:28.
24. Didelot C, Barberi-Heyob M, Bianchi A, Becuwe P, Mirjolet JF, Dauca M, et al. Constitutive NF-kappaB activity influences basal apoptosis and radiosensitivity of head-and-neck carcinoma cell lines. *Int J Radiat Oncol Biol Phys* 2001;**51**:1354–60.
25. Nakayama H, Ikebe T, Beppu M, Shirasuna K. High expression levels of nuclear factor kappaB, IkappaB kinase alpha and Akt kinase in squamous cell carcinoma of the oral cavity. *Cancer* 2001;**92**:3037–44.
26. Kumar A, Takada Y, Boriek AM, Aggarwal BB. Nuclear factor-kappaB: its role in health and disease. *J Mol Med* 2004;**82**:434–48.
27. Schwartz SA, Hernandez A, Mark Evers B. The role of NF-kappaB/IkappaB proteins in cancer: implications for novel treatment strategies. *Surg Oncol* 1999;**8**:143–53.
28. Yao J, Duan L, Fan M, Wu X. NF-kappaB signaling pathway is involved in growth inhibition, G2/M arrest and apoptosis induced by Trichostatin A in human tongue carcinoma cells. *Pharmacol Res* 2006;**54**:406–13.
29. Galleron S, Borderie D, Ponteziere C, Lemarechal H, Jambou M, Roch-Arveiller M, et al. Reactive oxygen species induce apoptosis of synoviocytes in vitro. Alpha-tocopherol provides no protection. *Cell Biol Int* 1999;**23**:637–42.
30. Rosato RR, Maggio SC, Almenara JA, Payne SG, Atadja P, Spiegel S, et al. The histone deacetylase inhibitor LAQ824 induces human leukemia cell death through a process involving XIAP down-regulation, oxidative injury, and the

acid sphingomyelinase-dependent generation of ceramide. *Mol Pharmacol* 2006;**69**:216–25.
31. Rosato RR, Almenara JA, Maggio SC, Coe S, Atadja P, Dent P, et al. Role of histone deacetylase inhibitor-induced reactive oxygen species and DNA damage in LAQ-824/fludarabine antileukemic interactions. *Mol Cancer Ther* 2008;**7**:3285–97.
32. Feng R, Oton A, Mapara MY, Anderson G, Belani C, Lentzsch S. The histone deacetylase inhibitor, PXD101, potentiates bortezomib-induced anti-multiple myeloma effect by induction of oxidative stress and DNA damage. *Br J Haematol* 2007;**139**:385–97.
33. Chen CS, Wang YC, Yang HC, Huang PH, Kulp SK, Yang CC, et al. Histone deacetylase inhibitors sensitize prostate cancer cells to agents that produce DNA double-strand breaks by targeting Ku70 acetylation. *Cancer Res* 2007;**67**:5318–27.